depending on the experimental condition [1-4]. The deficient line is black and the excess line white on photograph. The deficient-excess unindexed line is black on one side and white on the other side of the line. In the present work for the first time the contrast reversal along the unindexed line is obtained. The specimens were single crystalline silicon films prepared by chemical etching of bulky crystals. The transmission electron diffraction patterns were obtained in an EG-100M electron diffraction camera at an accelerating voltage of 100kV with the primary electron beam almost parallel to [111] axis. In the obtained Kikuchi patterns the unindexed line runs along the middle line of the Kikuchi band. The deficient unindexed line in the vicinity of the strong and spot reflections changes the contrast and transforms into excess line. The experimental conditions of unindexed line contrast reversal are founded. It is shown that the contrast is reversed when unindexed line passes through or in vicinity of an intense spot reflection. The contrast reversal of unindexed line is explained within the framework of the Kikuchi patterns formation mechanism with due regard for the double Kikuchi diffraction [5].

[1]   Pfister H. Ann. Phys.Lpz. 11, 239, 1953.
[2]   Uyeda R. and Nonoyama M. Japan. Journ. Appl. Phys. 4, 498, 1965.
[3]   Kainuma Y. and Kogiso M. Acta Cryst. A 24,1. 81. 1968.
[4]   Karakhanyan R.K. and Grigoryan P.A. Kristallografiya. 24, 1, p. 159. 1979.
[5]   Karakhanyan R.K., Aleksanyan P.L., Manucharova J.K. Phys. Stat. Sol.(a), 121, p.K1. 1990.

P19.03.06

Electron nanocrystallography: Advancements toward automated structure solution

Joseph T McKeown, John Spence
Arizona State University, Physics Department, P.O. Box 871504, Bateman Physical Sciences Center F Wing, PSF 470, Tempe, AZ, 85287, USA, E-mail：joseph.mckeown@asu.edu

The synthesis of new nanocrystalline structures demands new rapid methods of solving their crystal structures. Our goal is real-time structure solution at the electron microscope, based on automated acquisition of three-dimensional electron diffraction data with subsequent phasing of the data set and presentation of a unit-cell potential map that displays atomic positions and even species. To achieve this we must consider: 1) translation of the specimen during automated tilting; 2) automated recognition of zone-axis orientations; 3) multiple-scattering artifacts; 4) indexing methods; 5) absolute intensity scaling of the data; 6) scaling of data collected at different orientations; and 7) the phase problem. Initially, we have focused on issues 3) through 7) following manual acquisition of three-dimensional diffraction data from a known test crystal (the $MgAl_2O_4$ spinel structure). Data was collected by two techniques, both of which minimize multiple-scattering artifacts: precession electron diffraction (PED) and kinematic convergent beam electron diffraction (CBED) using an in-column Omega energy filter. After indexing and scaling, experimental structure-factor magnitudes were obtained from the patterns. These provide input to the charge-flipping algorithm [1], which works well with relatively poor-quality electron diffraction data or powder diffraction data [2], to solve the phase problem and obtain the correct crystal structure. Solutions for PED and kinematic CBED data are presented for comparison with each other and with simulations. Further development requires automated, scripted control of specimen tilt and data acquisition.

[1] G. Oszlanyi and A. Suto. Acta Cryst., A60, 134 (2004).

[2] J.S. Wu, J. Spence, M. O'Keeffe, and K. Leinenweber. Nat. Mater., 5, 647 (2006).

P19.03.07

Contribution of electron precession to the identification of a new zirconium hydride

Jean-Paul Morniroli[1], Zhao Zhao[1,2], Alexandre Legris[1], Martine Blat-Yrieix[2]
[1]Laboratoire de Metallurgie Physique et Genie des Materiaux, UMR CNRS 8517, USTL and ENSCL, Bat. C6, Cite Scientifique, Villeneuve d'Ascq, Nord, 59655, France, [2]EDF R&D, Centre des Renardieres, Ecuelles, 77818 Moret-sur-Loing Cedex, France, E-mail：Jean-Paul. Morniroli@univ-lille1.fr

A new metastable zirconium hydride designated as zeta-hydride, was identified and characterized in Zircaloy-4 alloys submitted to hydrogen cathodic charging or autoclave corrosion tests. Its crystal structure was obtained by combining TEM experiments and theoretical calculations. Using the electron precession microdiffraction technique, it was possible to identify slight differences of intensity between some weak extra reflections which prove that the highest "ideal" symmetry (the symmetry which takes into account both the position and the intensity of the reflections on a pattern) of this hydride is 3m. This symmetry is in agreement with a hexagonal lattice (with lattice parameters a=0.33 nm and c=1.029 nm) and with the Laue class -3m belonging to the trigonal crystal system. Then, the Zr_2H stoichiometric formula of the hydride was inferred from observations of plasmon peaks on EELS patterns. Finally, a structural model of the hydride, with space group P3m1, was deduced from ab-initio structure calculations and its validity was confirmed by subsequent dynamical simulations of the electron diffraction patterns.

P19.03.08

A study of structure properties of ZnS nano-crystals using electron crystallography

Jin-Gyu Kim[1], Seong-Je Park[1], Hyun-Min Park[2], Youn-Joong Kim[1]
[1]Korea Basic Science Institute, 52 Eoeun-dong, Yuseong-gu,, Daejeon, Daejeon, 305-333, Korea (S), [2]Korea Research Institute of Standards and Science, 209 Gajeong-ro, Yuseong-gu, Daejeon, 305-340, Korea (S), E-mail：jjintta@kbsi.re.kr

We have characterized the structure properties of two types of ZnS nano-crystals by electron crystallography. For determination of their initial structures, we have performed XRD analysis for ZnS crystals of 5 nm and 10 nm which were synthesized by same route. Their real crystallite sizes were about 5.9 nm and 8.1 nm and their crystal systems were hexagonal and cubic, respectively. Their quantitative structures, however, could not be determined because of their weak diffraction intensities. To overcome the intensity problem, the structure of ZnS nano-crystals was resolved by using EF-PED (Energy-Filtered Precession Electron Diffraction) and HREM (High Resolution Electron Microscopy) utilizing a HVEM (High

Voltage Electron Microscope). EF-PED data resulted in the basic crystallographic information of ZnS nano-crystals: $P63mc$, a = 3.83Å and c = 6.26Å; F-43m, a = 5.41Å, respectively. As a result of HREM analysis, their crystallite shapes were turned out to be nano-rods and nano particles, respectively and the nano-rod structure was elongated to the [001] direction. The size and shape dependency related to crystal structures of ZnS nano-crystals has been discussed.
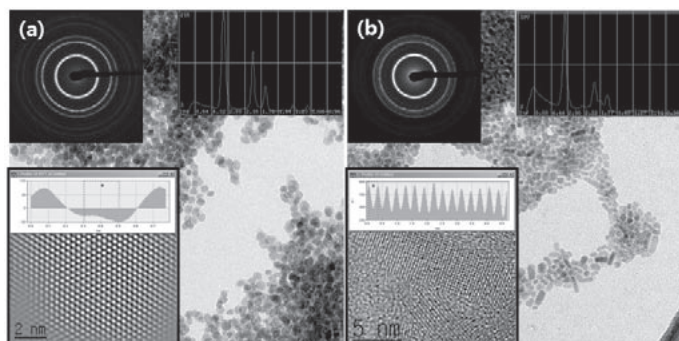

Fig. 1. EF-PED and HREM analysis of ZnS nano-crystals.
(a) Cubic structure of ZnS nano particles. (b) Hexagonal structure of ZnS nano-rods

Keywords: electron crystallography, energy-filtered precession electron diffraction, ZnS

P19.03.09

Electrostatic potential analysis of the orbital-ordered phase of spinel oxide FeCr$_2$O$_4$ using CBED

Daisuke Morikawa, Kenji Tsuda, Shintaro Ohtani, Takahisa Arima
Tohoku University, Institute of Multidisciplinary Reserch for Advanced Materials, 2-1-1 Katahira, Aoba-ku, Sendai, Miyagi, 980-8577, Japan, E-mail：morikawa@mail.tagen.tohoku.ac.jp

A structure analysis method using convergent-beam electron diffraction (CBED), which was developed by Tsuda and Tanaka[1,2], enables us to directly determine the electrostatic potential from a nanometer-scale specimen area. The electron density distribution can be also obtained from the electrostatic potential through the Poisson's equation. We have applied the method to a spinel oxide FeCr$_2$O$_4$, which undergoes a structural phase transformation at 135K from a cubic spinel structure of the high-temperature phase to a tetragonal structure of the low-temperature phase with Jahn-Teller(JT) distortion[3]. A ferro-type orbital-ordering of 3d electrons of Fe atoms is expected in the low-temperature JT-distorted phase of FeCr$_2$O$_4$[4]. FeCr$_2$O$_4$ single crystals were grown by the chemical vapor transport(CVT) method. Energy-filtered CBED patterns of the low-temperature phase were obtained at a specimens temperature of 90K using an energy-filter transmission electron microscope(EFTEM) JEM-2010FEF with an accelerating voltage of 100kV. Atom positions, Debye-Waller factors and low-order structure factors were refined by nonlinear least squares fitting between the experimental CBED patterns and dynamical diffraction calculations using an analysis software MBFIT[1]. The electrostatic potential and electron density distributions were reconstructed from the refined parameters. Clear anisotropy of the electrostatic potential has been found, which is attributed to the ferro-type ordering of the $3z^2$-r^2 orbitals of the Fe atoms.

References:[1]K. Tsuda & M. Tanaka, *Acta Cryst.* A**55**, 939-954(1999). [2]K. Tsuda et al., *Acta Cryst.* A**58**, 514-525(2002). [3]G.Shirane. *J. Appl. Phys.* **35**, 3(1964). [4]T.Arima et al., *J. Magn. Magn. Mat.* **310**, 807(2007).

Keywords: CBED, electrostatic potential, spinel

P19.03.10

Microstructural characterization of YPO$_4$: Li by transmission electron microscopy

Lucia Diaz-Barriga[1], Ivonne Rosales[2], Lauro Bucio[2]
[1]ESIQIE/ Instituto Politecnico Nacional, Metralurgia, Av.IPN S/N colonia Lindavista, MEXICO DF, DF, 07300, Mexico, [2]Instituto de Fisica, Universidad Nacional Autonoma de Mexico, Apdo. Postal 20-364, 01000 Mexico DF, Mexico, E-mail：luchell@yahoo.com

Xenotime YPO$_4$ is an yttrium phosphate with a tetragonal structure and can be doped by ions of diverse diameters in order to control its electrical conductivity. The purpose of this work is to present an study about the microstructural characterization of YPO$_4$ by electron transmission microscopy when this yttrium phosphate is doped with lithium. Samples were obtained by the following solid state reaction: Y$_2$O$_3$ +(NH$_4$)$_2$HPO$_4$-- >YPO$_4$:xLi Powder samples were studied in a JEOL 100 CX with point resolution of 2.7angstrom . Brigth field and Diffraction techniques were used to establish that YPO$_4$:xLi has an orthorhombic structure with lattice parameters: a=b= 9.7 angstrom and c= 6.01 angstrom ,this means that intersticial lithium ions can create a distortion in the tetragonal structure of yttrium phosphate.

Keywords: xenotime, orthorhombic yttrium phosphate, electron microscopy

P19.04.11

Determination of chiral indices of carbon nanotubes using electron diffraction pattern

Yohei Sato[1], Kenji Tsuda[1], Masami Terauchi[1], Yahachi Saito[2]
[1]Institute of Multidisciplinary Research for Advanced Materials, Tohoku University, 2-1-1 Katahira, Aoba-ku, Sendai, Miyagi, 980-8577, Japan, [2]Department of Quantum Engineering, Nagoya University, Furou-chou, Chikusa-ku, Nagoya 464-8603, Japan, E-mail：y-sato@tagen.tohoku.ac.jp

Carbon nanotubes (CNTs) show physical properties of a metal or a semiconductor depending on these structures. Thus, it is important to investigate the structure of a single CNT expressed by a chiral index (n, m) [1]. Transmission electron microscopy is a powerful tool to investigate structures of single CNTs. In the present study, the chiral indices are determined by using electron diffraction patterns obtained from single double-walled CNTs (DWCNTs) and single single-walled CNTs (SWCNTs). Electron diffraction patterns were obtained from 200 nm areas containing a single DWCNT or SWCNT by using a transmission electron microscope of JEM2010 at an accelerating voltage of 100 kV. Intensities of the diffraction patterns were recorded on imaging plates. Determination process of chiral indices is as follow. 1.The chiral angles and diameters of the CNT are estimated from the diffraction patterns. 2.The chiral indices (n, m) of the CNT are estimated from the angles and the diameters. 3.Diffraction patterns of chiral indices (n, m) were simulated using a simulation program "MBFIT" [2, 3]. 4.The simulated diffraction patterns are compared with the experimental patterns. 5.Chiral indices (n, m) were determined from the best agreement between the experimental and the simulated patterns. The determination of chiral indices enables us to calculate the joint densities of states of the CNTs and to compare electron energy-loss spectra of the CNTs with joint density of states of the CNTs calculated from chiral indices (n, m).

P19